Special Issue of the 6th International Congress & Exhibition (APMAS2016), Maslak, Istanbul, Turkey, June 1–3, 2016

Physical Properties and Microstructural Characterization of Mechanically Alloyed and Sintered W–2wt%B_4C–$x$wt%C (x = 0, 0.25, 0.5, 1) Composites

S. Sönmez[a,b,*] and M.L. Öveçoğlu[a]

[a]Istanbul Technical University, Materials Science and Engineering Faculty, Ayazağa Campus, Particulate Materials Laboratories, 34469 Istanbul, Turkey

[b]Hakkari University, Engineering Faculty, Department of Mechanical Engineering, 30000 Hakkari, Turkey

Mechanical alloying processes were carried out in a Spex mixer/mill to synthesize W–2wt% B_4C–$x$wt% C (x = 0, 0.25, 0.5, 1) powders for durations of 1 and 9 h in argon atmosphere. Mechanically alloyed powders were consolidated into green compacts by uniaxial cold press under 500 MPa and solid phase sintered at 1770 °C under hydrogen and argon atmospheres for 1 h and 5 h. Effects of milling duration as well as C addition on the microstructural and mechanical properties of the sintered W–2wt% B_4C–$x$wt% C composite samples were investigated. The microstructural and mechanical characterizations of the sintered samples were carried out by scanning electron microscope, energy dispersive X-ray spectroscopy, X-ray diffraction, and Vickers hardness analyses. Density measurements and hardness measurements of the sintered samples were also carried out.

DOI: 10.12693/APhysPolA.131.193

PACS/topics: 81.05.Ni

1. Introduction

Tungsten (W) has the highest melting point (varies between 3387 °C and 3422 °C) of all elements except carbon. With a density of 19.25 g/cm^3, W is also among the heaviest metals. W matrix composites reinforced with carbide, boride, and oxide particles are quite attractive for different structural applications and for some nuclear applications at high temperatures and at severe service conditions [1–6].

Tungsten borides such as W_2B, WB, and W_2B_5 have high hardness, heat resistance, and wear resistance which makes them attractive candidate materials for severe service conditions [7, 8]. High energy mechanical milling is a very effective process for synthesis of metal/ceramic composite powders and for producing powders with nanocrystalline structures [9]. W–B_4C–C systems can be utilized to synthesize tungsten borides. Boron carbide (B_4C) is a ceramic material which has strong covalent bonds. Consequently, it is extremely hard, with low density, high elastic modulus, and low sinterability [3].

The aim of the present investigation was to study the effects of carbon rate on the properties of mechanically alloyed and sintered W–2wt% B_4C–$x$wt%C (x = 0, 0.25, 0.5, 1) composites. Laser diffraction size analysis, nanosizer, X-ray diffraction (XRD), and scanning electron microscopy (SEM) were used to characterize the powders and density and microhardness measurements were made on sintered composites from these materials.

*corresponding author; e-mail: sultansonmez@itu.edu.tr

2. Materials and method

Elemental tungsten (W) powders (Eurotungstene™, 99.9% purity, 42 μm average particle size) as the matrix of the powder composite and boron carbide (B_4C) powders (Alfa Aesar™, 99.9% purity, 7 μm average particle size) reinforcing particles were utilized in this investigation. Moreover, 0–0.25–0.5–1wt% graphite powders (Alfa Aesar™, 99.9% purity, 21 µm average particle size) were added to each batch as a process control agent (PCA) to eliminate cold welding between powder particles and thereby to prevent agglomeration.

W, B_4C, and C powders were blended to constitute the compositions of W–2wt%B_4C–$x$wt%C (x = 0, 0.25, 0.5, 1) which were mechanically alloyed for 1 and 9 h. High-energy milling experiments were carried out in a Spex™ DuoMixer/Mill 8000D using a tungsten carbide (WC) vial and WC balls (6.35 mm in diameter) as milling media. The ball-to-powder weight ratio (BPR) was 10:1. To avoid oxidation during mechanical alloying (MA), the vials were sealed inside a Plaslabs™ glove box under Ar gas (99.995% purity). Mechanically alloyed powders were cold-pressed at a pressure of 50 MPa in an APEXTM™ 3010/4 uni-action hydraulic press. Pressed samples were sintered in a Linn™ high temperature hydrogen furnace at 1770 °C under inert Ar (introduced between room temperature to 600 °C and 1100–1770 °C), and reducing H_2 (introduced between 600 and 1100 °C) gas flowing conditions for 1 h and 5 h.

Morphological characterizations were carried out using JEOL™ JCM-6000 Neoscope Benchtop scanning electron microscope attached with JEOL™ WX-36210DPP EDS unit (energy dispersive spectrometer) with an accelerating voltage 15 kV. Microstructural characterizations were carried out using a Bruker™ D8 Advance XRD

(Cu K_α radiation) and SEM. Sintered densities were measured by using the Archimedes density method. The Vickers microhardness tests were conducted on sintered samples using a Shimadzu™ microhardness tester under a load of 500 g for 15 s. Microhardness test result for each sample is the arithmetic mean of at least 10 successive indentations and standard deviations.

3. Results and discussion

Table I shows that the compositions and relative Archimedes density of the W–2wt%B_4C–$x$wt%C (x = 0, 0.25, 0.5, 1) composites. Relative Archimedes density values generally increase with increasing MA durations. At the same time relative Archimedes density values increase with increase of sintering time. Maximum relative Archimedes density value shown in W2B0.5C–MA9h–S5h composite, while minimum relative Archimedes density values shown W2B0.25C–MA1h–S1h composite (Table I).

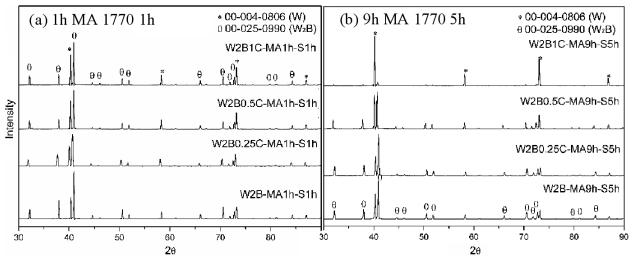

Fig. 1. XRD patterns of the sintered bulk composites: (a) 1h MA 1770 1h, (b) 9h MA 1770 5h.

X-ray diffraction patterns of W–2wt%B_4C–$x$wt%C (x = 0, 0.25, 0.5, 1) sintered bulk composites for different milling times are shown in Fig. 1a and b. The XRD patterns of sintered composites reveal the presence of the characteristic peaks of the W and W_2B phase. W_2B and W peaks can be seen and characteristic peaks of B_4C and C do not appear. With increase in milling time W_2B peak intensities reduced, excluding 1 h MA'd and 1 h sintered composites. With increase C rate W_2B peak intensities reduced drastically, especially include 1wt% C composites. With increase of C rate and sintering time increased B and C solubility in the W matrix WC peaks do not appear, probably, due to the low amount. As seen in Fig. 2a–d, increase of milling time caused the dispersion of the carbide phases more homogeneously. However, after 1 h MA time, microstructures are very heterogeneous and porous. After 9 h MA duration, microstructures have homogeneous phases. After 5 h sintering time, microstructures are more homogeneous and dense than 1 h. EDS point analysis used to figure out the B and C phases dispersed in W matrix which can be seen in Fig. 2e–h and Table II. This analysis supported decarburization and formation of W_2B phase. At grain boundaries, even so B_4C and WC phases present, B_4C decarburized on a large scale. Increasing with weight percent of C, decarburization rate decrease.

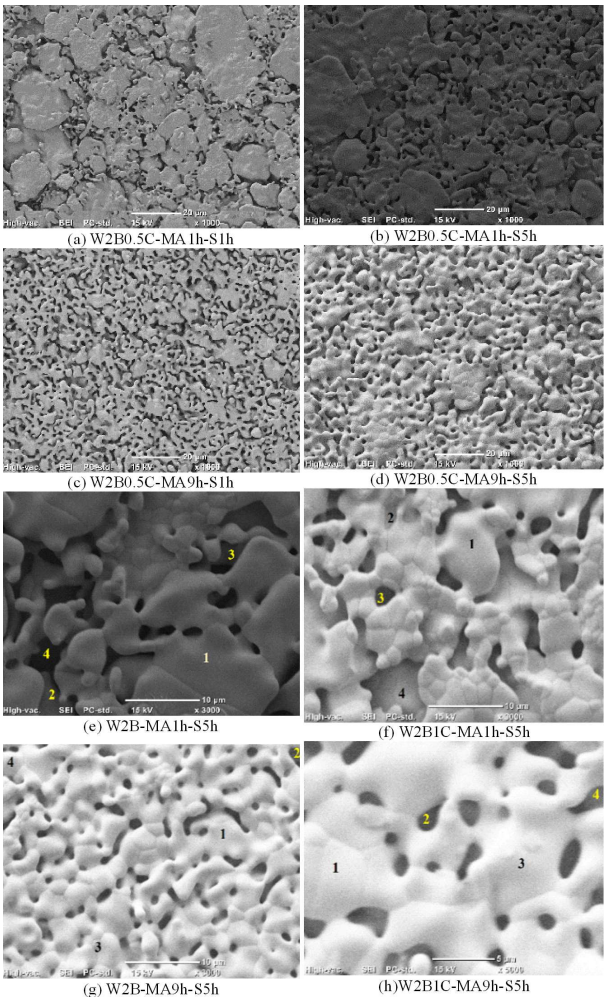

Fig. 2. SEM microstructures and EDS point analyses of the sintered composites: (a) W2B0.5C–MA1h–S1h, (b) W2B0.5C–MA1h–S5h, (c) W2B0.5C–MA9h–S1h, (d) W2B0.5C–MA9h–S5h, (e) W2B–MA1h–S5h, (f) W2B1C–MA1h–S5h, (g) W2B–MA9h–S5h, (h) W2B1C–MA9h–S5h.

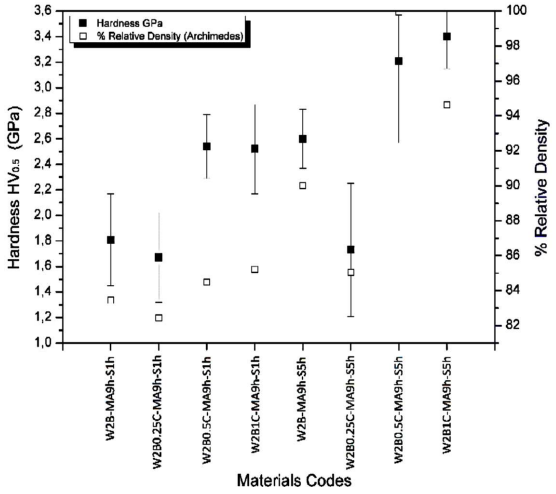

Fig. 3. Hardness of the sintered composites.

In Fig. 3, the results of microhardness values are given. The minimum hardness values are obtained after 1 h milling time for the W2B0.25C–MA9h–S1h sintered composite. Hardness values are proportional to the milling time and increase of C rate, but at 0.25wt%C it decreases, then starts to increase again. The hardness values of W2B0.5C–MA9h–S5h and W2B1C–MA9h–S5h are similar to each other.

TABLE I

The composition [wt%] and relative density [%] of the studied W–2wt%B_4C–$x$wt%C (x = 0, 0.25, 0.5, 1) composites.

Material code	W	B_4C	C	MA time [h]	Sintering time [h]	r.d.
W2B-MA1h-S1h	98	2	–	1	1	73.35
W2B-MA1h-S5h	98	2	–	1	5	92.82
W2B-MA9h-S1h	98	2	–	9	1	83.45
W2B-MA9h-S5h	98	2	–	9	5	90.01
W2B0.25C-MA1h-S1h	97.75	2	0.25	1	1	72.38
W2B0.25C-MA1h-S5h	97.75	2	0.25	1	5	83.76
W2B0.25C-MA9h-S1h	97.75	2	0.25	9	1	82.44
W2B0.25C-MA9h-S5h	97.75	2	0.25	9	5	85.04
W2B0.5C-MA1h-S1h	97.5	2	0.5	1	1	78.25
W2B0.5C-MA1h-S5h	97.5	2	0.5	1	5	94.10
W2B0.5C-MA9h-S1h	97.5	2	0.5	9	1	84.48
W2B0.5C-MA9h-S5h	97.5	2	0.5	9	5	99.95
W2B1C-MA1h-S1h	97	2	1	1	1	78.69
W2B1C-MA1h-S5h	97	2	1	1	5	88.89
W2B1C-MA9h-S1h	97	2	1	9	1	85.23
W2B1C-MA9h-S5h	97	2	1	9	5	94.63

TABLE II

EDS point analyses of the 5 h sintered W–2wt%B_4C–$x$wt%C (x = 0, 0.25, 0.5, 1) composites.

EDS point		W2B-MA1h-S5h		W2B1C-MA1h-S5h		W2B-MA9h-S5h		W2B1C-MA9h-S5h	
		[wt%]	[at%]	[wt%]	[at%]	[wt%]	[at%]	[wt%]	[at%]
	B	0.78	6.92	5.02	26.17	12.92	50.56	1.25	10.54
1	C	5.62	44.56	10.19	47.82	8.93	31.46	5.71	43.31
	W	93.60	48.52	84.79	26.0	78.14	17.98	93.05	46.15
	B	2.22	16.37	9.31	33.39	7.44	33.26	1.41	13.78
2	C	6.67	44.18	15.74	50.81	11.29	45.39	3.60	31.63
	W	91.11	39.45	74.95	15.80	81.27	21.35	94.99	54.58
	B	12.24	37.81	9.40	41.67	–	–	1.73	11.37
3	C	17.79	49.47	9.30	37.13	14.03	71.41	9.20	54.29
	W	69.98	12.72	81.30	21.20	85.97	28.29	89.07	34.34
	B	12.92	50.56	1.72	9.76	8.17	50.22	19.14	47.32
4	C	8.93	31.46	12.04	61.47	8.70	30.65	19.67	43.78
	W	78.14	17.98	86.24	28.76	83.13	19.13	61.19	8.90

4. Conclusion

1. Relative densities are proportional to the milling time. Increase of milling time also increases the relative densities.
2. In sintered composites, W_2B phases intensity decreases with increase of C rate and sintering time, excluding 0.25wt%C composite.
3. Carbon rate has an important effect on decarburization, while increasing C rate, decarburization rate decreases.
4. Carbide phases located at the grain boundaries which can be seen according to the SEM/EDS analyses. B and C phases dispersed more homogeneously in W matrix, increasing with MA duration.
5. EDS analysis proves that increasing milling time is very important to have homogeneous mechanical properties after sintering.
6. After 9 h MA duration, W2B1C–MA9h–S5h has the highest hardness values (3.4 GPa), while W2B0.25C–MA9h–S1h has the least (1.65 GPa).

Acknowledgments

The authors would like to thank the Scientific Research Projects Coordination Unit (BAP) of Istanbul Technical University for partial funding of this investigation with the project number 39825.

References

[1] S. Coşkun, A. Genç, M.L. Öveçoglu, *Met. Mater. Int.* **19**, 533 (2013).

[2] A. Genç, S. Coşkun, M.L. Öveçoglu, *J. Alloys Comp.* **508**, 162 (2010).

[3] N. Ünal, M.L. Öveçoğlu, *Powd. Met.* **52**, 254 (2009).

[4] M. Rieth, et al., *J. Nucl. Mater.* **432**, 482 (2013).

[5] M. Zibrov, M. Mayer, L. Gao, S. Elgeti, H. Kurishita, Yu. Gasparyan, A. Pisarev, *J. Nucl. Mater.* **463**, 1045 (2015).

[6] A.B. Tuğrul, E. Demir, O. Yılmaz, S. Sönmez, M.L. Öveçoglu, B. Büyük, *Acta Phys. Pol. A* **129**, 724 (2016).

[7] S. Stadler, R.P. Winarski, J.M. MacLaren, D.L. Ederer, J. van Ek, A. Moewes, M.M. Grush, T.A. Callcott, R.C.C. Perera, *J. Electron. Spectrosc. Relat. Phenom.* **110**, 75 (2000).

[8] C. Suryanarayana, *Prog. Mater. Sci.* **46**, 1 (2001).

[9] W.Z. Zhang, J.E. Zhou, Q.X. Sheng, G. Ran, P.L. Li, *Mater. Sci. Eng. A* **379**, 148 (2004).